

Brief Report

Phytomelatonin Regulates Keratinocytes Homeostasis Counteracting Aging Process

Francesca Ferri ¹, Fabio Olivieri ¹, Roberto Cannataro ², Maria Cristina Caroleo ^{2,3,*} and Erika Cione ^{2,3}

¹ EFFEGI LAB Srl Lavis (TN), 38015 Lavis TN, Italy; francesca.ferri@effegilab.com (F.F.); scientifico@effegilab.com (F.O.)

² GalaScreen Srl University of Calabria-Italy, 87036 Calabria, Italy; r.cannataro@gmail.com (R.C.); erika.cione@unical.it (E.C.)

³ Department of Pharmacy, Health and Nutritional Sciences, Department of Excellence 2018-2022, University of Calabria, Rende (CS), 87036 Rende, Italy

* Correspondence: mariacristinacaroleo@virgilio.it; Tel.: +39-098-449-3193; Fax: +39-098-449-3107

Received: 25 March 2019; Accepted: 16 April 2019; Published: 18 April 2019



Abstract: Phytomelatonin (PM) gained the greatest interest for its application in agriculture and its use to improve human health conditions. PM based supplement has been shown to possess antioxidant capabilities because it functions as a free radical scavenger. Reactive Oxygen Species (ROS), induced by both intrinsic (peroxide production) and extrinsic (UV-radiation) factors are biochemical mediators crucial in skin aging. Skin aging is also regulated by specific microRNAs (miRs). Herein we have shown the effect of PM free radical scavengers on the human keratinocyte cell line HaCat and on ROS formation induced by both extrinsic and intrinsic factors as well as their capability to positively modulate a member of the hsa-miR-29 family linked to aging. Our result highlights the regulatory role of PM for the keratinocytes homeostasis.

Keywords: phytomelatonin; skin aging; microRNAs

1. Introduction

Phytomelatonin (PM) is a plant derivative, also called N-acetyl-5-methoxytryptamine, known to be synthesized by plants in hard climate conditions. PM plant distribution is ubiquitous and in different parts of plants, including the leaves, roots, fruits, and seeds [1]. At the moment, two different aspects of PM have gained the greatest interest: (i) its application in agriculture; and (ii) its use to improve human health conditions. Indeed, PM and melatonin share both chemical structure and biological properties. Amongst these properties is the capability to act as an antioxidant and to function as a free radical scavenger [1]. Recent data clearly indicate that supplementation in PM with nutraceuticals is related to an increase in serum antioxidant capability [2,3]. Antioxidant defense against Reactive Oxygen Species (ROS) are biochemical mediators crucial in the skin aging. In fact, previous studies have pointed out that continuous exposure to ROS can stimulate through the antioxidant system destruction, melanogenesis, wrinkle formation and skin aging [4]. The skin aging process can be induced by intrinsic and extrinsic factors. This latter is due to the environment, as exposure to ultraviolet (UV) radiation contributes to up to 80% to skin aging [5]. Intrinsic skin aging occurs because of cumulative endogenous damage due to the continual formation of ROS which is also essential for biological functions [6,7]. Therefore, they are generated constantly during normal cellular metabolism and are typically eliminated from the body through the antioxidant defense system [7]. Indeed, antioxidant defense system dysfunction and the imbalance between ROS formation and removal can cause cells damage by free radical reactions. MicroRNAs (miRs) as biomarkers of pathology (mainly in cancer)

and regulators of gene expression have been well recognized from end to end of abundant publications over the last 10 years [8]. Their role in the aging process and the oxidative stress is emerging [9]. Amongst these miRs, the physiological role of the hsa-miR-29 family in the control of cell-extracellular matrix and aging is very interesting [9–11].

Herein we have shown the effect of PM free radical scavengers on the human keratinocyte cell line HaCat and on ROS formation induced by both extrinsic and intrinsic factors, as well as their capability on a member of hsa-miR-29 family linked to aging.

2. Materials and Methods

2.1. *Phytomelatonin Extraction and Cell Culture*

Phytomelatonin oil (PM) obtained from EFFEGI LAB Srl was solubilized in several organic solvents e.g., -dimethyl sulfoxide; -ethyl glycol; -acetonitril; -diethyl glycol at 1:1 and 1:10 dilutions. Moreover, -propylene glycol and -glycerol were also tested at at 1:1 and 1:2 dilutions without success. Positive results were achieved by 1,2-dimethoxyethane at both 1:1 and 1:10 dilutions but when it was added to the culture media, after 30 min a phase separation was observed. Therefore, PM oil was extracted in ethyl acetate and then lyophilized and re-dissolved in DMSO and used as weight/volume.

The human immortalized keratinocyte cell line, HaCaT, were grown in 25 cm² flask (Bibby, Milan, Italy). Cells were cultured at 37 °C, 5% CO₂, in Dulbecco's modified Eagle's medium (DMEM) supplemented with 10% fetal bovine serum (FBS) and 1% antibiotics (10,000 µg/mL streptomycin and 10,000 units/mL penicillin). The cells number was estimated with a Burkert camera. For each treatment, cells were plated in a 96 and or 24 well plate or in 100-mm polystyrene dish (Falcon, Becton-Dickinson, Lincoln Park, NJ, USA).

2.2. *Cell Viability Assay*

Cell viability was determined by the MTT assay, measuring the reduction of 3-(4,5-dimethylthiazol-2-yl)-2,4-diphenyltetrazolium bromide (MTT) by mitochondrial succinate dehydrogenase, as previously described [12]. The MTT enters the cells and passes into the mitochondria where it is reduced to an insoluble, colored, formazan product. The amount of color produced is directly proportional to the number of viable cells. HaCat cells were incubated with a different amount of PM (from 0 to 200 µg) in 96-well-plates for 24 h. At the time of assay, MTT (10 µL, 5 mg/mL in PBS) was added to each well and incubated for 3 h at 37 °C. The medium was then carefully aspirated, and DMSO (100 µL) was added to solubilize the colored formazan product, agitating the plates for 5 min on a shaker. The absorbance of each well was measured with a microtiter plate reader (Synergy H1 by BioTeck). The optical density (OD) was calculated as the difference between the absorbance at the reference wavelength (690 nm) and the absorbance at the test wavelength (570 nm). Percent viability was calculated as (OD of treated sample/OD of control) ×100.

2.3. *DAPI and Fluorescent Staining*

Change in morphology for nuclei and cytoskeleton remodeling were assessed by 4,6-diamidino-2-phenylindole (DAPI) and phalloidin. HaCat cells were grown on a cover glass lip into 24 well plate and treated with PM at 10 µg for 24 h. The cells were then fixed in 4% paraformaldehyde and the fluorescence was imaged using confocal FV-3000 Olympus microscope (Tokyo, Japan). For measuring intracellular ROS and mitochondrial membrane potential (MMP), PM pre-treatment at 10 µg for 6 h was performed. Then, 5 µM of CellRox Deep Red ($\lambda = ex/em = 640/665$) dye was added after H₂O₂ 500 µM exposure and incubated for further 30 min. Then, cells were exposed to UV for 30 min and mitochondrial membrane potential was assessed by adding 2 µM MitoTracker Red CMXRos dye ($\lambda = ex/em = 579/599$) for further 15 min (outside the UV lamp). The cells were then fixed in 4% paraformaldehyde and the fluorescence was imaged using confocal FV-3000 Olympus microscope and Leica DVM6 microscope (Wetzlar, Germany), respectively.

2.4. MicroRNAs Extraction and Loop Primer Method

MicroRNA was isolated using a PureLink™ miRNA Isolation Kit (K1570-01 Ambion by Life Technologies, Waltham, Massachusetts, U.S.) as already described [13]. The quantification of miRNA was performed with a method termed looped primer RT-PCR, following the protocol. Initially, 10 ng of total RNA was subjected to reverse transcription polymerase chain reaction using the TaqMan MicroRNA Reverse Transcription kit (Thermo Fisher Scientific, Waltham, Massachusetts, U.S.), according to the manufacturer's protocol. The thermocycling conditions were: 30 min at 16 °C, followed by 30 min at 42 °C, 5 min at 85 °C and 5 min at 4 °C.

2.5. Quantitative Real Time PCR (qRT-PCR)

The quantitative real-time polymerase chain reaction (qRT-PCR) was performed using TaqMan Universal PCR Master Mix Kit (Thermo Fisher Scientific, Waltham, Massachusetts, U.S.) according to the manufacturer's protocol and the equipment QuantumStudio3™ Real-Time PCR Systems. The thermocycling conditions were: 95 °C for 10 min, and 40 cycles of 15 s at 95 °C, followed by 1 min at 60 °C. After finalization of the qRT-PCR experiments, the average values of the cycle threshold (Ct) of the reactions in triplicate were determined. The relative expression of the miR target was plotted as follows: 40 total qRT-PCR cycle - Ct target miR. This difference (Δ ct) was plotted directly as already described [14].

2.6. In Silico Analysis for Predicted Target Genes

In order to identify genes as the target of the hsa-miR tested, we performed in silico analysis. The in silico identification of the target genes was performed using miRWalk, miRDB, and miR target link human databases as well as a string database.

2.7. Statistical Analysis

Data were analyzed using the ANOVA method followed by the Bonferroni's test. The differences were considered significant for values of $P < 0.05$ (*), $P < 0.01$ (**), and $P < 0.001$ (***)

3. Results and Discussion

Melatonin is an evolutionary ancient hormone that belongs to both, animals and plants. Although they have the same chemical structure, the hormone present in the latter is indicated as phytemelatonin (PM). At present, in the cosmetic industry phytochemicals are widely used [15], while phyto-stem-cells and phytohormones application is an emerging field [16]. In this view herein we tested the effect of PM on human keratinocytes cell biology. As shown in Figure 1, the exposure of cell culture to five and 200 µg of PM did not affect cell viability compared to the control (DMSO-vehicle). Instead a significant increase of cell viability was observed in HaCaT cell line treated with PM in the range between 10 to 50 µg.

Our results revealed that this compound affected cell viability in a dose-response fashion and strongly suggested the involvement of the receptor mechanisms. Indeed, the higher amount used at 200 µg drastically decreased cell viability. This mechanism was probably due to the melatonergic receptors (MTRs) desensitization [17]. Likewise, the dose of 5 µg was unable to activate MTRs. Based on our results, the dose chosen for the other in vitro test was 10 µg of PM.

Cytoskeletal remodeling and keratinocytes terminal differentiation are markers of skin regeneration [18]. In this view, evaluation of cell morphology was assessed by fluorescence microscopy. Change in cell morphology gaging cytoskeletal remodeling and nuclear lobe formation was tested by phalloidin-stained F-actin and DAPI, respectively. In Figure 2, keratinocytes cultured without (Panel A) and with PM (Panel B) cytoskeletal remodeling was observed. The yellow arrows in Figure 2 panel A indicate that the F actin filaments show a centromedian cellular localization. In the presence of PM for 24 h, the isoform F of the actin show a cortical localization near to the plasma membrane as

indicated with the white arrows (Panel B). Terminal differentiation of keratinocytes was assessed by changes in nuclear morphology. The lobed (half-moon) nucleus are typical of terminal differentiation. In the presence of PM for 24 h, a significant number of lobed nuclei are shown by orange arrows (Panel D) compared to the control (Panel C). Indeed, in our set of experiments PM induced a re-localization of isoform F of the actin near to the plasma membrane as well as lobed (half-moon) nucleus shape typical of terminal differentiation.

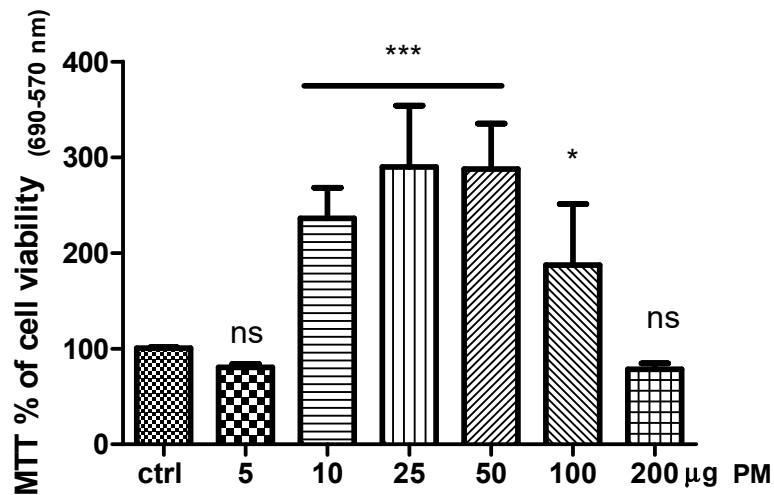


Figure 1. Dose response of phytomelatonin (PM) in human keratinocytes cell viability. A significant increase of the cell vitality was appreciated when exposed to PM in the range between 10 to 50 µg (** $P < 0.0001$) and at 100 µg (* $P < 0.05$) compared to the control (DMSO-vehicle).

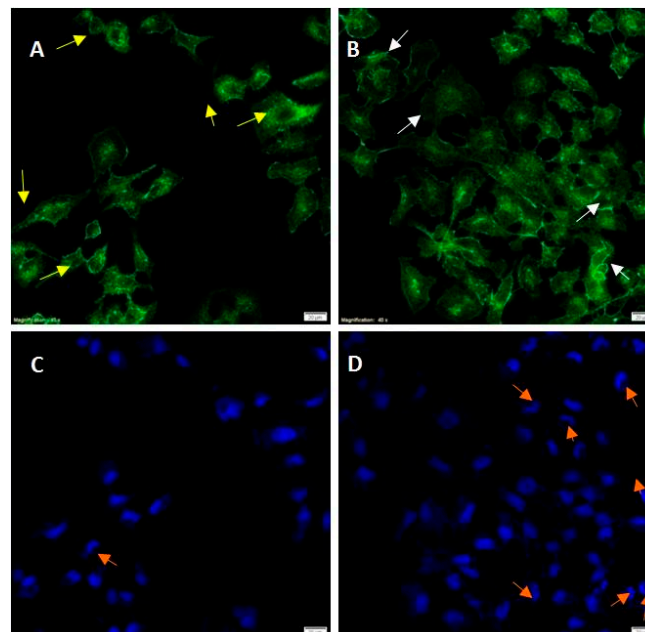


Figure 2. Cytoskeletal remodeling and nuclear lobe formation upon PM. Representative images of phalloidin-stained F-actin in keratinocytes cultured without (A) and with PM (B) for 24 h ($n = 3$ independent experiments). Scale bars: 20 µm. Representative images of DAPI-stained nuclei keratinocytes cultured without (C) and with PM (D) for 24 h ($n = 3$ independent experiments). Scale bars: 20 µm.

A crucial aspect of skin aging promotion is the role played by both ROS generation (intrinsic aging factor) and UV exposure which leads to ROS production (extrinsic and intrinsic aging factors) [19].

It is well known that the formation of ROS takes place predominantly on mitochondria and that mitochondrial membrane potential (MMP) upon UV radiation is impaired generating free radicals [20].

In this concern, the estimation of MMP which lead to ROS generation was performed by fluorescence microscopy. The red-fluorescent MitoTracker Red CMXRos dye stains mitochondria in live cells and its accumulation dependent by MMP. The keratinocytes were treated for 6 h with 10 μg PM. As shown in Figure 3, the exposure of the HaCaT cell line to 10 μg PM induced a significant decrease in the mitochondrial membrane potential (Panel B) compared to control cultures (Panel A) when exposed to a UV lamp at 254 nm (UVC spectrum to avoid vitamin D synthesis). In Panel C, graph box plot of red dots pixel analysis ($*** P = 0.0002$) is shown.

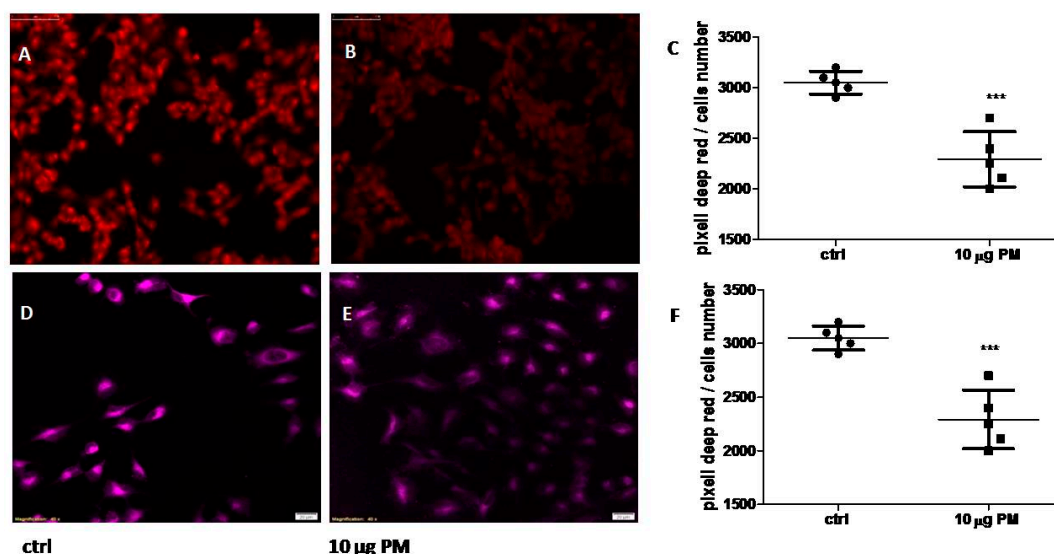


Figure 3. Mitochondrial membrane potential and intracellular reactive oxygen species (ROS) upon PM. Representative images of mitochondrial membrane potential (MMP) stained in keratinocytes cultured without (A) and on 10 μg of PM (B) for 24 h. Scale bars: 20 μm (C). Quantification of the average cell area pixel for red staining keratinocytes. Data in C represent mean \pm sd of $n = 3$ independent experiments ($*** P = 0.0002$). Representative images of intrROS stained in keratinocytes cultured without (D) and on 10 μg of PM (E) for 24 h. Scale bars: 20 μm . (F) Quantification of average cell area pixel for deep red staining keratinocytes. Data in F represent mean \pm sd of $n = 3$ independent experiments ($*** P = 0.0002$).

The physiological processes due to mitochondrial activity can synergize with intracellular ROS, thus inducing cellular aging [20,21].

Therefore, we further evaluated the intracellular reactive oxygen species (intrROS) formation, treating keratinocytes for 6 h with 10 μg of PM and then exposing the cellular layer to H_2O_2 500 μM for 30 min. The specific dye CellRox Deep Red revealed that PM significantly decreased intrROS formation, as shown in Figure 3 Panel E, compared to the control counterpart (Panel D), suggesting a potent scavenging action of PM. In Panel F, a graph box plot of deep-red dots pixel analysis ($*** P = 0.0002$) is shown.

Thus, as well as acting on cytoskeletal remodeling and keratinocytes terminal differentiation, which indicate skin regeneration [22], in our set of experiments PM was able to counteract both extrinsic and intrinsic insult acting as a free radical scavenger.

The antioxidant defense system dysfunction and imbalance between ROS formation and removal can cause cells to influence gene expression, a process in which microRNAs (miRs) are well recognized to be crucial regulators [8].

The involvement of MiRs in the aging process and oxidative stress is emerging [9] and the role of the hsa-miR-29 family in the control of cell-extracellular matrix, aging and skin regeneration is exciting [9–11,22].

In this concern, using qRT-PCR analysis revealed low levels of hsa-miR-29a-3p in the control samples compared to in PM treated ones. As shown in Figure 4 Panel A, the increase of this miR upon PM 24-hour treatment was about 50%.

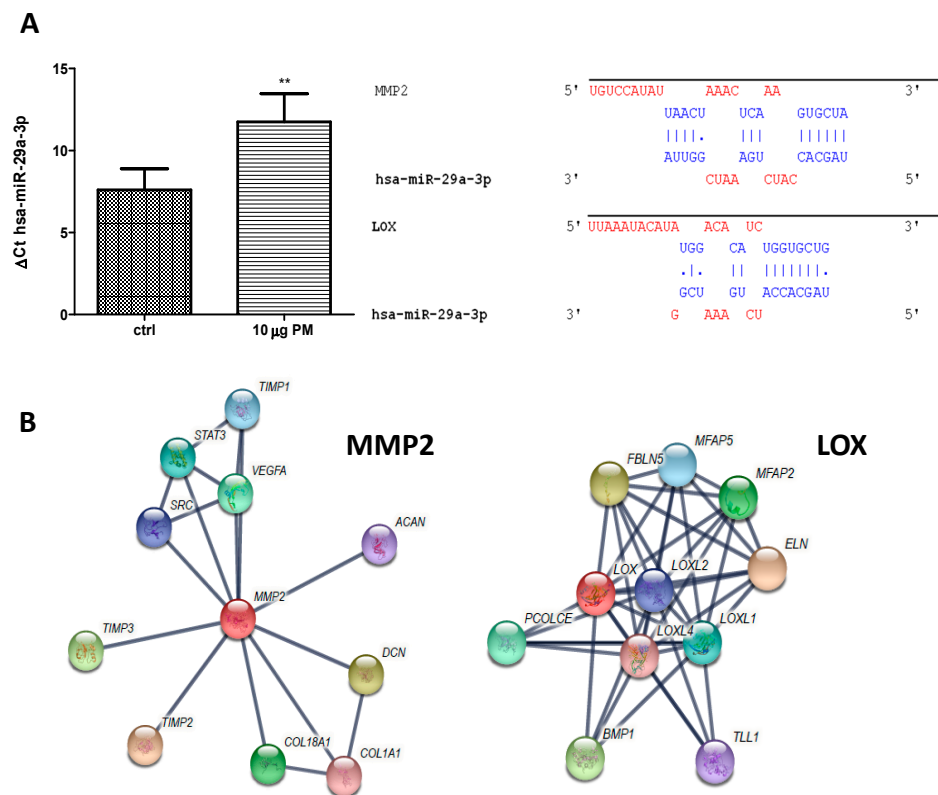


Figure 4. PM induce hsa-miR29-3p expression (A) has-miR-29a-3p expression without and with PM and its mRNAs interaction. (B) String data protein MMP2 and LOX interactions.

As a result, we showed the effect of PM on the increase of hsa-miR-29a-3p, which is able to counteract the aging process [11].

In order to predict the target genes of hsa-miR-29a-3p and identify possible genes involved in keratinocytes homeostasis, we used three different tools. Eighty predicted target genes were found for hsa-miR-29a-3p. Of these, the genes linked to keratinocytes homeostasis were chosen, as shown in Table 1 using miR target link.

Table 1. Validated target genes with high score interaction linked to keratinocytes homeostasis for hsa-miR-29a-3p according to the miR target link database.

Target Gene	Gene Name	miRTarBase ID
MMP2	matrix metalloproteinase 2	MIRT053580
LOX	lysyl oxidase	MIRT437550

The in silico analysis, revealed that validated hsa-miR-29a-3p target genes are involved in keratinocyte homeostasis. The genes affected by this miR were mainly two: (i) MMP2 (collagenase type 2 or matrix metalloproteinase 2) and (ii) LOX (lysyl oxidase).

The physical interactions between miR and the mRNAs and string protein interactions, both experimentally validated, are depicted in Figure 4A,B, respectively. The target matrix metalloproteinase (MMP) 2 gene is very interesting.

MMPs are collagenase able to degrade collagen and elastin fibers in the connective tissue of the skin. In effect, collagen and elastin degradation has been reported through both, MMP-1 and MMP-2 [23].

Likewise, excessive ROS generation by both intrinsic or extrinsic factors leads to DNA damage in normal cells and an increase of the MMP level, which can promote skin aging [23].

Besides that, this miR is able to target also the lysyl oxidase (LOX) enzyme that strongly impairs terminal differentiation when expressed during the late keratinocytes differentiation process [24].

In conclusion, our study demonstrated that PM affected several aspects of human keratinocytes biology ranging from the promotion of cell survival to a protective effect against oxidative damage. In addition, our results highlight for the time an epigenetic modulation of this compound, paving the way for the use of PM as an advanced cosmetic tool in the improvement of skin performance.

Author Contributions: Conceptualization, F.F.; Formal analysis, R.C. and E.C.; Funding acquisition, F.F.; Methodology, R.C. and E.C.; Project administration, F.O.; Supervision, M.C.C.; Writing—original draft, M.C.C. and E.C.; Writing—review & editing, F.F., F.O., R.C., M.C.C. and E.C.

Acknowledgments: We acknowledge M. Badolato and F. Aiello (University of Calabria, Italy) for PM oil extraction and Nuclear Magnetic Resonance (NMR) analysis before and after extraction procedure.

Conflicts of Interest: F.F. and F.O. are CEO and scientific coordinator of EFFEGI LAB Srl, respectively.

References

- Bhattacharjee, A. Phytomelatonin: A comprehensive literature review and recent advance on medicinal meadow. *Int. J. Hydrol.* **2018**, *2*, 1. [[CrossRef](#)]
- Benot, S.; Gobema, R.; Reiter, R.J.; Garcia-Mauriño, S.; Osuna, C.; Guerrero, J.M. Physiological levels of melatonin contribute to the antioxidant capacity of human serum. *J. Pineal Res.* **1999**, *27*, 59–64. [[CrossRef](#)]
- Kanwar, M.K.; Yu, J.; Zhou, J. Phytomelatonin: Recent advances and future prospects. *J. Pineal Res.* **2018**, e12526. [[CrossRef](#)]
- Kim, D.S.; Jeon, B.K.; Mun, Y.J.; Kim, Y.M.; Lee, Y.E.; Woo, W.H. Effect of Dioscorea aimadoimo on anti-aging and skin moisture capacity. *J. Orient. Physiol. Pathol.* **2011**, *25*, 425–430.
- Chung, J.H.; Seo, J.Y.; Choi, H.R.; Lee, M.K.; Youn, C.S.; Rhie, G.-E.; Cho, K.H.; Kim, K.H.; Park, K.C.; Eun, H.C. Modulation of Skin Collagen Metabolism in Aged and Photoaged Human Skin In Vivo. *J. Investig. Dermatol.* **2001**, *117*, 1218–1224. [[CrossRef](#)] [[PubMed](#)]
- Park, J.S. Walnut husk ethanol extract possess anti-oxidant activity and inhibitory effect of matrix metalloproteinase-1 expression induced by tumor necrosis factor alpha in human keratinocyte. *Kor J. Aesthet Cosmetol.* **2013**, *11*, 715–719.
- Shon, M.-S.; Lee, Y.; Song, J.-H.; Park, T.; Lee, J.K.; Kim, M.; Park, E.; Kim, G.-N. Anti-aging Potential of Extracts Prepared from Fruits and Medicinal Herbs Cultivated in the Gyeongnam Area of Korea. *Prev. Nutr. Food Sci.* **2014**, *19*, 178–186. [[CrossRef](#)] [[PubMed](#)]
- Catalanotto, C.; Cogoni, C.; Zardo, G.; Taguchi, Y.-H. MicroRNA in Control of Gene Expression: An Overview of Nuclear Functions. *Int. J. Mol. Sci.* **2016**, *17*, 1712. [[CrossRef](#)]
- Yaribeygi, H.; Atkin, S.L.; Sahebkar, A. Potential roles of microRNAs in redox state: An update. *J. Cell. Biochem.* **2018**, *120*, 1679–1684. [[CrossRef](#)] [[PubMed](#)]
- Kriegel, A.J.; Liu, Y.; Fang, Y.; Ding, X.; Liang, M. The miR-29 family: Genomics, cell biology, and relevance to renal and cardiovascular injury. *Physiol. Genom.* **2012**, *44*, 237–244. [[CrossRef](#)]
- Li, T.; Yan, X.; Jiang, M.; Xiang, L. The comparison of microRNA profile of the dermis between the young and elderly. *J. Dermatol. Sci.* **2016**, *82*, 75–83. [[CrossRef](#)] [[PubMed](#)]
- Perri, M.; Pingitore, A.; Cione, E.; Vilardi, E.; Perrone, V.; Genchi, G. Proliferative and anti-proliferative effects of retinoic acid at doses similar to endogenous levels in Leydig MLTC-1/R2C/TM-3 cells. *Biochim. Biophys. Acta General Subj.* **2010**, *9*, 993–1001. [[CrossRef](#)] [[PubMed](#)]
- Perri, M.; Caroleo, M.C.; Liu, N.; Gallelli, L.; De Sarro, G.; Kagechika, H.; Cione, E. 9-cis Retinoic acid modulates myotrophin expression and its miR in physiological and pathophysiological cell models. *Exp. Cell* **2017**, *354*, 25–30. [[CrossRef](#)] [[PubMed](#)]

14. Weber, J.A.; Baxter, D.H.; Zhang, S.; Huang, D.Y.; Huang, K.-H.; Lee, M.-J.; Galas, D.J.; Wang, K.; Butterfield, A.M.; Luan, P.; et al. The MicroRNA Spectrum in 12 Body Fluids. *Clin. Chem.* **2010**, *56*, 1733–1741. [[CrossRef](#)] [[PubMed](#)]
15. Barbulova, A.; Colucci, G.; Apone, F. New Trends in Cosmetics: By-Products of Plant Origin and Their Potential Use as Cosmetic Active Ingredients. *Cosmetics* **2015**, *2*, 82–92. [[CrossRef](#)]
16. Trehan, S.; Michniak-Kohn, B.; Beri, K. Plant stem cells in cosmetics: Current trends and future directions. *Futur. Sci. OA* **2017**, *3*, FSO226. [[CrossRef](#)] [[PubMed](#)]
17. Nita, M.; Grzybowski, A. The Role of the Reactive Oxygen Species and Oxidative Stress in the Pathomechanism of the Age-Related Ocular Diseases and Other Pathologies of the Anterior and Posterior Eye Segments in Adults. *Oxidative Med. Cell. Longev.* **2016**, *2016*, 1–23. [[CrossRef](#)]
18. Botchkareva, N. MicroRNA/mRNA regulatory networks in the control of skin development and regeneration. *Cell Cycle* **2012**, *11*, 468–474. [[CrossRef](#)]
19. Waterhouse, N.J.; Goldstein, J.C.; Von Ahsen, O.; Schuler, M.; Newmeyer, D.D.; Green, D.R. Cytochrome C Maintains Mitochondrial Transmembrane Potential and Atp Generation after Outer Mitochondrial Membrane Permeabilization during the Apoptotic Process. *J. Cell Boil.* **2001**, *153*, 319–328. [[CrossRef](#)]
20. Liu, J.; Clough, S.J.; Hutchinson, A.J.; Adamah-Biassi, E.B.; Popovska-Gorevski, M.; Dubocovich, M.L. MT1 and MT2 Melatonin Receptors: A Therapeutic Perspective. *Annu. Pharmacol. Toxicol.* **2015**, *56*, 361–383. [[CrossRef](#)]
21. Fletcher, D.A.; Mullins, R.D. Cell mechanics and the cytoskeleton. *Nat. Cell Boil.* **2010**, *463*, 485–492. [[CrossRef](#)]
22. Park, S.-Y.; Byun, E.J.; Lee, J.D.; Kim, S.; Kim, H.S. Air Pollution, Autophagy, and Skin Aging: Impact of Particulate Matter (PM10) on Human Dermal Fibroblasts. *Int. J. Mol. Sci.* **2018**, *19*, 2727. [[CrossRef](#)]
23. Pittayapruerk, P.; Meehansan, J.; Prapapan, O.; Komine, M.; Ohtsuki, M.; Maki, M. Role of Matrix Metalloproteinases in Photoaging and Photocarcinogenesis. *Int. J. Mol. Sci.* **2016**, *17*, 868. [[CrossRef](#)]
24. Mainzer, C.; Remoué, N.; Molinari, J.; Rousselle, P.; Barricchello, C.; Sommer, P.; Sigaudou-Roussel, D.; Debret, R.; Lago, J.C. In vitro epidermis model mimicking IGF-1-specific age-related decline. *Exp. Dermatol.* **2018**, *27*, 537–543. [[CrossRef](#)]



© 2019 by the authors. Licensee MDPI, Basel, Switzerland. This article is an open access article distributed under the terms and conditions of the Creative Commons Attribution (CC BY) license (<http://creativecommons.org/licenses/by/4.0/>).